

GNSS Reflectometry Global Ocean Wind Speed Estimation Based on CyGNSSMsa

Weimin Chen^{1*}, Bin Wang¹, Dongmei Song^{1,2}

¹College of Oceanography and Space Informatics, China University of Petroleum (East China), Qingdao, China

²Laboratory for Marine Mineral Resources, Qingdao National Laboratory for Marine Science and Technology, Qingdao, China

Email: *chenwmupc@163.com

How to cite this paper: Chen, W.M., Wang, B. and Song, D.M. (2025) GNSS Reflectometry Global Ocean Wind Speed Estimation Based on CyGNSSMsa. *Journal of Computer and Communications*, 13, 190-200. <https://doi.org/10.4236/jcc.2025.136013>

Received: May 18, 2025

Accepted: June 27, 2025

Published: June 30, 2025

Abstract

GNSS Reflectometry (GNSS-R) technology utilizes existing navigation satellite signals as opportunistic microwave illumination sources, eliminating the need for dedicated transmitters and thereby significantly reducing hardware costs. Benefiting from the global coverage of navigation constellations, GNSS-R enables worldwide sea surface wind monitoring with superior spatiotemporal resolution. The acquired Delay-Doppler Maps (DDMs) encode sea surface roughness characteristics near the specular reflection point, which are intrinsically modulated by wind-driven capillary waves. We proposed CyGNSSMsa employs CyGNSSnet's dual-branch framework for preliminary feature extraction from DDM and auxiliary parameters, followed by multihead self-attention (MSA) mechanisms to decipher long-range dependencies within fused feature representations. Multi-scale feature fusion is achieved through residual connections across hierarchical network layers, culminating in precise wind speed regression via multilayer perceptrons. Experimental validation demonstrates CyGNSSMsa's performance with an RMSE of 1.345 m/s, achieving simultaneous improvements in both accuracy and systematic bias mitigation.

Keywords

GNSS-R, CYGNSS, Ocean Wind Speed

1. Introduction

Sea surface wind speed (SSWS), as a pivotal parameter in oceanographic research, governs sea surface roughness through air-sea interactions and modulates marine dynamic processes. Accurate SSWS monitoring holds critical operational value for maritime navigation, fisheries management, and disaster mitigation, yet conventional in-situ measurements from buoys and coastal stations suffer from spa-

tial coverage constraints that hinder large-scale maritime applications. Although satellite-based remote sensing technologies (e.g., microwave radiometers and synthetic aperture radar) have enabled synoptic wind field observations, their operational implementation faces dual challenges: prohibitive costs in maintaining dense satellite constellations and inherent limitations in temporal revisit frequency and spatial coverage continuity, particularly compromising monitoring effectiveness in critical sea areas.

The comprehensive constellation deployment of Global Navigation Satellite Systems (GNSS), encompassing the American GPS, Russian GLONASS, European Galileo, and Chinese BDS systems, has collectively established a global, all-weather microwave signal network. GNSS-transmitted L-band navigation signals function as ubiquitous and cost-free microwave sources, characterized by strong atmospheric penetration capability with minimal attenuation from clouds, rain, or snow, thereby enabling persistent observational capabilities under diverse weather conditions. Unlike synthetic aperture radar (SAR) requiring active electromagnetic emission, GNSS reflectometry (GNSS-R) exploits passively reflected L-band signals from the sea surface, effectively repurposing navigation satellites as bistatic remote sensing transmitters. This innovative approach has catalyzed extensive applications in Earth observation, including but not limited to sea surface wind speed retrieval, altimetry, sea ice thickness quantification, marine oil spill monitoring, and soil moisture inversion.

The scattering of GNSS signals over the sea surface induces measurable modulations in signal power, time delay, and Doppler shift, which exhibit intrinsic correlations with sea surface roughness. Given the stable transmission power of GNSS signals and the quasi-constant dielectric properties of seawater, DDM variations are predominantly governed by wind-driven alterations in sea surface roughness, thereby establishing a robust physical foundation for high-precision wind speed inversion. Systematic decoding of scattering signatures embedded in Delay-Doppler Maps (DDMs) enables the development of quantitative inversion models linking sea surface roughness parameters to wind speed magnitudes, achieved through advanced feature extraction algorithms and electromagnetic scattering theory.

Substantial scholarly efforts have validated the feasibility of sea surface wind speed (SSWS) retrieval using Delay-Doppler Maps (DDMs). Research on DDM-based SSWS inversion has evolved into two distinct methodological frameworks: feature engineering and data-driven approaches. Early-stage investigations focused on DDM feature extraction and empirical model formulation: Clarizia *et al.* [1] pioneered the development of Geophysical Model Functions (GMFs) incorporating leading edge slope (LES) and normalized bistatic radar cross section (NBRCS) parameters, coupled with Minimum Variance Estimators (MVEs) for wind speed retrieval, which established the foundational framework for feature-driven methodologies. Subsequent advancements introduced geometric correction factors including incidence angle calibration and range-compensated gain (RCG) adjustments [2]-[4], achieving root mean square error (RMSE) optimization to the 2.0

m/s level, marking significant progress in precision.

The integration of deep learning with remote sensing technologies has revolutionized data-driven methodologies, where end-to-end feature learning substantially enhances model representation capabilities. Liu *et al.* [5] achieved a breakthrough in wind speed retrieval (RMSE = 1.79 m/s) by employing Multilayer Perceptron (MLP) to synergistically fuse DDM-derived parameters (mean power, LES) with observational geometry parameters (incidence angle). Subsequent innovations by Asgarimehr, Liu, and collaborators [6] [7] further expanded the feature space through the incorporation of auxiliary parameters such as antenna gain patterns and satellite attitude data, while pioneering neural network architectures to autonomously extract latent features from raw DDM observations, thereby advancing inversion accuracy.

Cross-domain model migration from computer vision and natural language processing has opened new frontiers for GNSS-R wind speed retrieval. Asgarimehr *et al.* [8] developed CyGNSSnet, a dual-branch heterogeneous network architecture, where a convolutional neural network (CNN) branch extracts local spatio-temporal features from DDM delay-Doppler domains while a parallel fully-connected branch integrates auxiliary parameters (signal-to-noise ratio, incidence angle), achieving an RMSE of 1.36 m/s. Subsequently, Guo *et al.* [9] enhanced this framework by incorporating a cumulative distribution function (CDF) matching module that aligns probability distributions to mitigate systematic biases at high wind speeds, reducing full-range RMSE (0 - 25 m/s) to 1.53 m/s. Diverging from CNNs' localized receptive fields, Zhao *et al.* [10] proposed DDM-former a transformer-based architecture employing stacked multi-head self-attention (MSA) layers in decoder modules to capture global long-range dependencies within DDM's 2D delay-Doppler distributions. This pure DDM-input approach attained 1.43 m/s RMSE without auxiliary parameters, demonstrating the superiority of attention mechanisms in feature integration through its paradigm shift from "manual feature fusion" to "data-driven global modeling".

Building upon the demonstrated efficacy of CyGNSSnet and DDM-former in establishing nonlinear DDM-to-wind speed mappings through deep learning, we propose CyGNSSMsa—a novel neural architecture synergistically integrating CyGNSSnet's framework with self-attention mechanisms. This hybrid model enhances feature perception by deploying attention modules to refine features extracted from DDMs by CyGNSSnet. Multi-level residual connections enable progressive fusion of hierarchical features across scales, while a final Multilayer Perceptron (MLP) stage optimizes the regression for high-precision wind speed inversion. The architecture systematically combines local receptive field advantages of CNNs with global context modeling through attention, achieving comprehensive feature representation.

2. Experimental Datasets

2.1. Data Description

The experimental study utilized the CYGNSS Version 3.2 dataset spanning 31

consecutive days from January 1 to 31, 2024. For DDM data processing, four primary parameters were selected: 1) bistatic radar cross section (BRCS) representing true scattering area, 2) effective scattering area derived from GPS waveform and scattering surface calculations, 3) simulated power corresponding to actual sensor-measured power, and 4) raw counts as uncalibrated power measurements. Additionally, two auxiliary parameters were incorporated: leading edge slope (LES) describing the rising edge slope of the power waveform, and normalized bistatic radar cross section (NBRCS) quantifying scattering cross-section magnitude near the specular reflection point—both established parameters in wind speed inversion studies. This multi-parameter configuration ensures comprehensive characterization of both physical scattering mechanisms and sensor-specific responses (Figure 1).

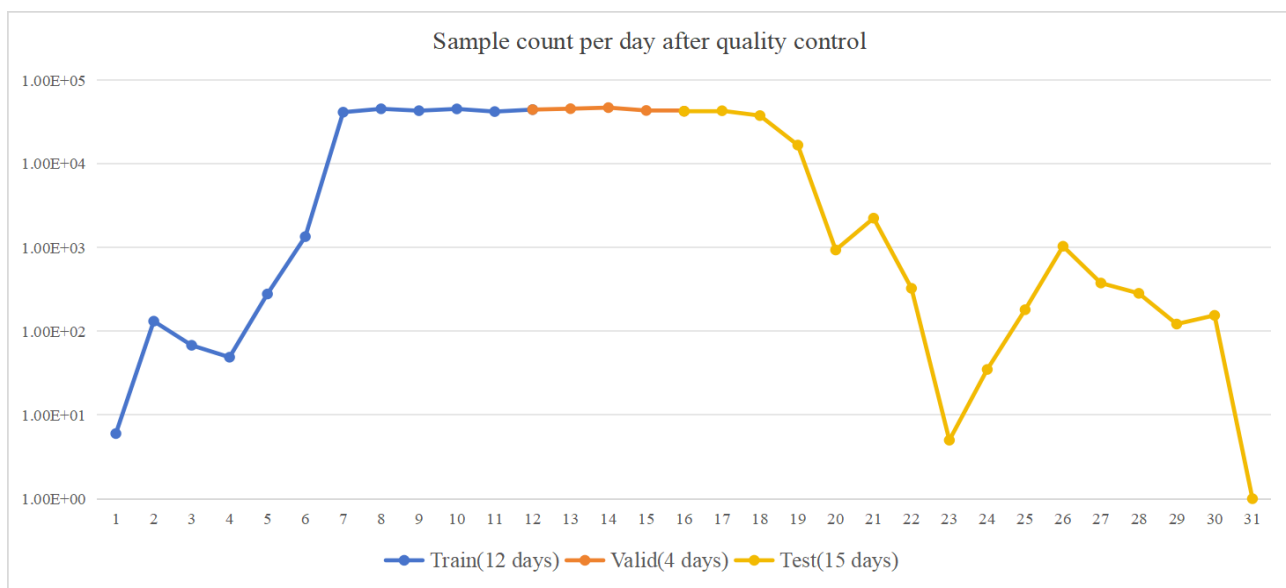


Figure 1. Sample count per day after quality control.

The reference wind speed data were obtained from the European Centre for Medium-Range Weather Forecasts (ECMWF) ERA5 reanalysis dataset, providing hourly temporal resolution and $0.25^\circ \times 0.25^\circ$ spatial resolution. To achieve precise spatiotemporal collocation between CYGNSS observations and ERA5 wind fields, the ERA5 data were processed through linear temporal interpolation to match CYGNSS measurement timestamps, coupled with spatial bilinear interpolation across the 0.25° grid to align with specular reflection point coordinates. This two-stage interpolation protocol ensures sub-hour temporal synchronization and sub-grid spatial correspondence, generating reference wind speed values with ≤ 0.5 -hour temporal offset and < 12.5 km spatial uncertainty for robust GNSS-R model training and validation.

2.2. Quality Control

The relatively low power of navigation signals reaching Earth's surface renders

GNSS-R observations susceptible to microwave interference, potentially compromising data integrity. To mitigate low-quality data impacts, we implemented a multi-criteria quality control protocol leveraging CYGNSS-defined quality flags, signal-to-noise ratio (SNR), and range-corrected gain (RCG). The institutional quality flags effectively eliminate artifacts caused by sensor anomalies and system noise, while SNR quantifies DDM signal clarity through noise-floor comparison. RCG, defined as the ratio between specular point gain and signal propagation path loss, serves as a critical indicator of geometric observation validity. Our filtering strategy systematically removed data samples exhibiting: 1) questionable quality flags, 2) $\text{SNR} \leq 3$ dB (insufficient signal dominance), or 3) $\text{RCG} \geq 10$ (excessive path attenuation).

3. Methodology

3.1. CyGNSSMsa Model

Recent advancements in deep learning for sea surface wind speed retrieval using CYGNSS DDM data have yielded multiple sophisticated architectures [8]-10]. Among these, CyGNSSNet employs a dual-branch convolutional neural network (CNN)-based architecture to process auxiliary parameters and DDM features independently, providing flexible extensibility for multi-modal data integration. In contrast, DDM-former leverages self-attention mechanisms to establish global dependencies across entire DDM matrices, demonstrating exceptional proficiency in aggregating long-range scattering characteristics. These architectures fundamentally aim to establish robust feature-to-wind speed mappings through distinct learning paradigms: CyGNSSNet emphasizes localized spatial pattern extraction via convolutional kernels, whereas DDM-former excels in capturing inter-channel correlations through transformer-based attention weight allocation. Comparative analyses reveal that while CyGNSSNet's modular design facilitates incremental parameter integration, DDM-former's encoder-decoder structure achieves superior performance ($\text{RMSE} \leq 1.43$ m/s) through holistic DDM interpretation, substantiating the transformative potential of attention mechanisms in geophysical parameter inversion tasks.

Building upon the architectural merits of both CyGNSSNet and DDM-former, we propose CyGNSSMsa—a hybrid deep learning framework for wind speed retrieval. The model initiates with parallel feature extraction streams: auxiliary parameters (e.g., incidence angle, SNR) are processed through fully connected layers to generate metadata embeddings, while a convolutional extracts localized features from raw DDM matrices. These heterogeneous features undergo channel-wise concatenation and dimensionality alignment before being fed into multi-head self-attention (MSA) layers, which establish global dependencies across the fused feature space. The refined representations are subsequently regressed to wind speed values through a multilayer perceptron (MLP) with residual connections, enabling nonlinear mapping optimization. This hierarchical architecture synergistically combines CNN's local feature sensitivity with transformer-based

global context modeling, while maintaining auxiliary parameter compatibility through adaptive fusion layer (Figure 2).

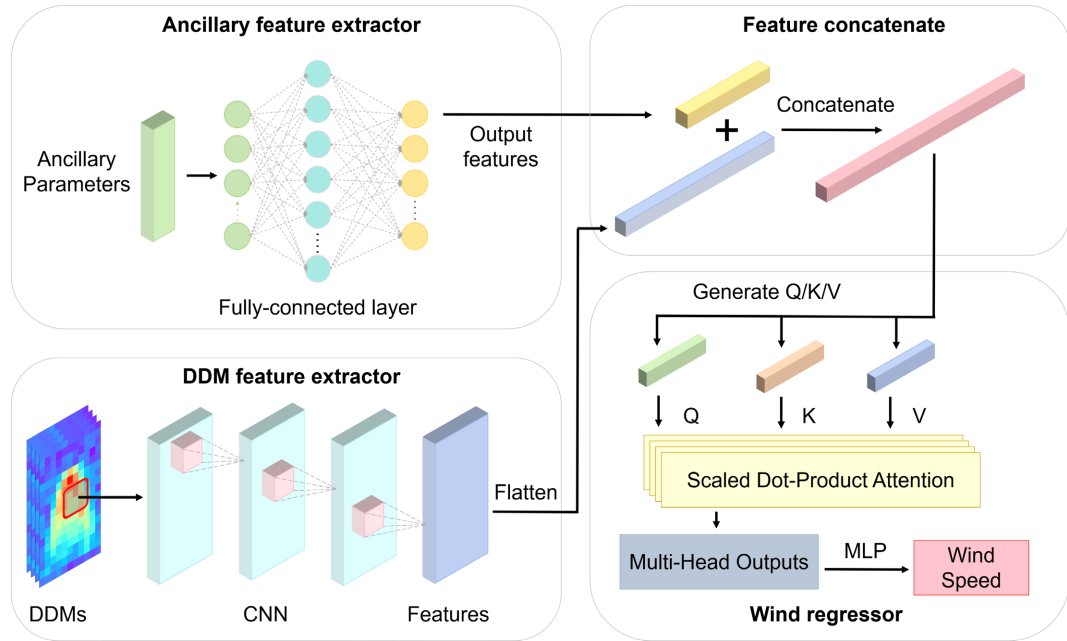


Figure 2. General structure of CyGNSSMs.

The experimental DDM datasets maintain a uniform dimensionality of [4, 11, 17], corresponding to channels ($C = 4$), height ($H = 11$), and width ($W = 17$), representing four DDM parameters across 11 delay bins and 17 Doppler bins. Auxiliary parameters (LES and NBRCS) are formatted as [2, 1] tensors. The processing pipeline initiates with convolutional operations on the input tensor using 3×3 kernels to extract local spatiotemporal features, followed by batch normalization to stabilize layer input distributions through mini-batch statistics (mean μ , variance σ^2):

$$BN(x) = \frac{x - \mu}{\sqrt{\sigma^2 + \epsilon}} \quad (1)$$

where ϵ denotes numerical stability factor. Rectified Linear Unit (ReLU) activation then introduces nonlinearity:

$$Relu(x) = \max(x, 0) \quad (2)$$

Subsequent max pooling (2×2 window) enhances feature discriminability through spatial subsampling. To enable hierarchical feature fusion while mitigating gradient vanishing, residual connections implement identity mapping:

$$Res(x) = F(x) + x \quad (3)$$

where F represents stacked convolution-normalization-activation operations. This architecture preserves multi-scale information flow from shallow to deep layers.

For the auxiliary data processing stream, we implement a dedicated neural architecture comprising a fully connected layer with 48 hidden units to transform

input parameters, followed by dropout regularization with a rate of 0.3 to mitigate overfitting risks. The linear transformation stage projects the [2, 1] auxiliary tensor into a 48-dimensional latent space through weight matrix multiplication:

$$\text{Liner}(x) = F(x, W_{48}) \quad (4)$$

where $W_{48} \in \mathbb{R}^{48 \times 2}$ denotes the learnable weight matrix and $b \in \mathbb{R}^{48}$ the bias vector. Subsequently, dropout stochastically deactivates 10% of neurons during training via random sampling.

Following feature concatenation between DDM-derived and auxiliary embeddings, we implement positional encoding using PyTorch's native functionalities to inject spatial-temporal awareness into the fused feature tensor. The concatenated features undergo sinusoidal positional encoding along the Doppler-delay dimensions:

$$\begin{aligned} PE(pos, 2i) &= \sin(pos / 10000^{2i/d}) \\ PE(pos, 2i+1) &= \cos(pos / 10000^{2i/d}) \end{aligned} \quad (5)$$

where pos denotes position index and i the dimension. Subsequent layer normalization stabilizes feature distributions across dimensions through per-feature mean (μ) and standard deviation (σ) normalization:

$$\text{LayerNorm}(x) = \gamma \cdot \frac{x - \mu}{\sigma} + \beta \quad (6)$$

with learnable parameters γ (scale) and β (shift). The normalized features then enter multi-head self-attention (MSA) layers comprising 4 parallel attention heads. Each head computes query-key-value projections:

$$\text{Attention}(Q, K, V) = \text{softmax}\left(\frac{QK^T}{\sqrt{d_k}}\right)V \quad (7)$$

where $d_k = 64$ denotes key dimension. The concatenated multi-head outputs form position-aware contextual representations, enabling global dependency modeling across Doppler-delay domains.

The refined features from the multi-head self-attention (MSA) layers are subsequently fed into a multilayer perceptron (MLP) to generate wind speed estimates

The specific structure of the model is as follows:

3.2. Model Validation

For comprehensive performance evaluation, we conducted comparative analyses against three established GNSS-R wind speed retrieval approaches (Figure 3): 1) the conventional Minimum Variance Estimator (MVE) [1] utilizing normalized bistatic radar cross section (NBRCS) and leading edge slope (LES) features derived from DDM data; 2) the convolutional neural network-based CyGNSSnet [8] employing dual-branch architecture for DDM-auxiliary feature fusion; and 3) the attention-driven DDM-former [10] achieving auxiliary-free inversion through multi-head self-attention layers. The MVE method implements physics-based wind speed

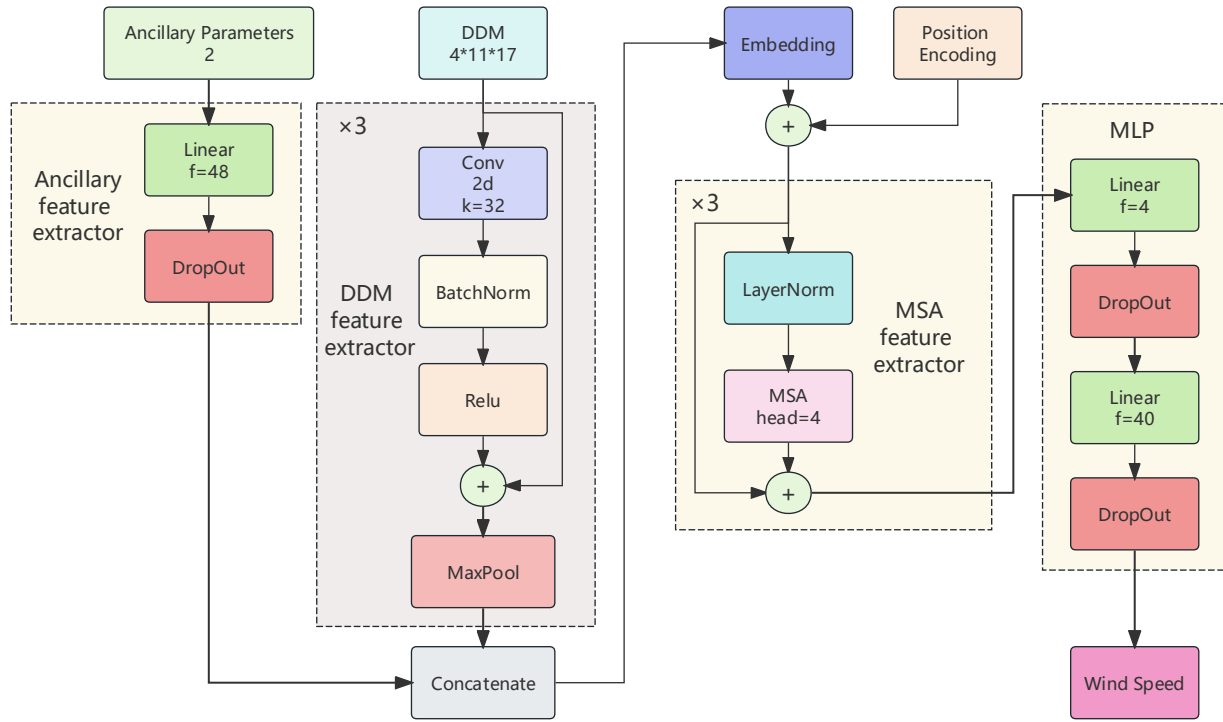


Figure 3. Specific structure of CyGNSSmsa for the experiment.

estimation via empirically calibrated geophysical model functions (GMFs), while CyGNSSnet adopts hybrid feature engineering through parallel CNN and MLP pathways. In contrast, DDM-former leverages global attention mechanisms to establish direct DDM-to-wind speed mappings without auxiliary parameter dependence. Model performance was quantitatively assessed using root mean square error (RMSE, m/s) and bias (m/s) metrics, calculated as:

$$RMSE(y, y_{real}) = \sqrt{\frac{1}{n} \sum_{i=1}^n (y - y_{real})^2} \quad (8)$$

$$Bias(y, y_{real}) = \frac{1}{n} \sum_{i=1}^n (y - y_{real}) \quad (9)$$

where y_{real} is the reference wind speed obtained from ERA5 and y is the predicted wind speed from the model output.

3.3. Training Details

The model was trained on a single NVIDIA GeForce RTX 2060s GPU. The framework used was pytorch, the optimiser used was Adam, the learning rate was 0.001, the sample batch size was 4096, and a total of 100 rounds were run to train the model.

4. Results and Discussion

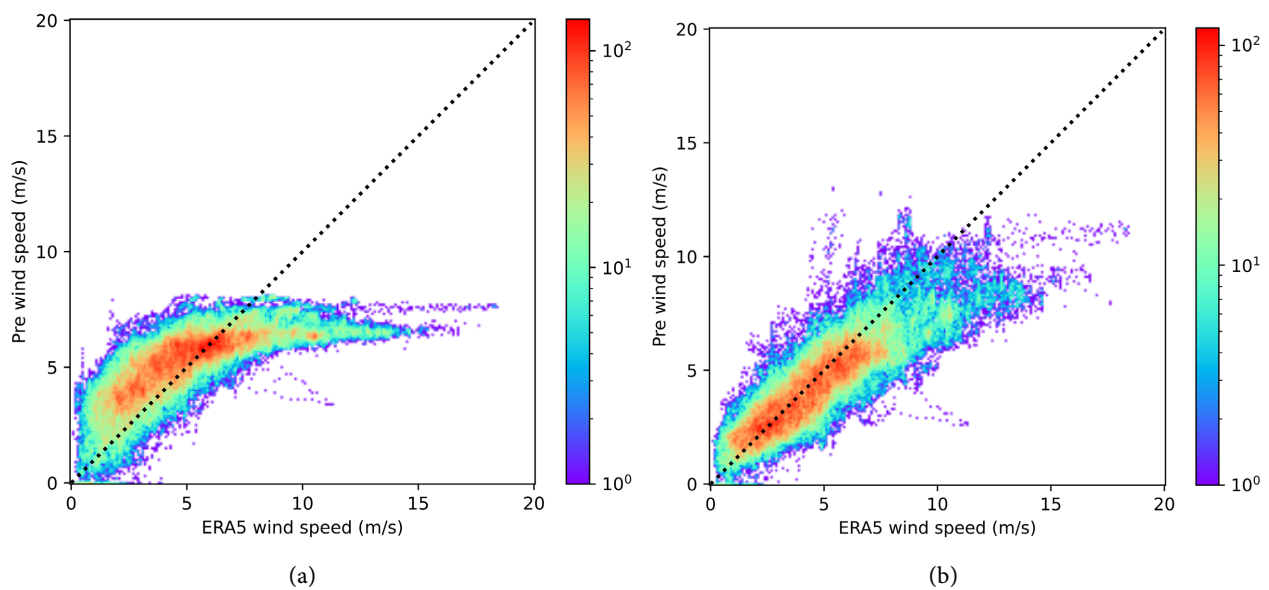
The overall RMSE of the methods and the RMSE in different wind speed bands

are shown in **Table 1**.

Table 1. RMSE statistics for baselines and proposed model with different wind intervals

Architecture	All samples	≤4 m/s		4 - 8 m/s		8 - 12 m/s		12 - 16 m/s		>16 m/s	
	RMSE (m/s)	RMSE (m/s)	Bais (m/s)	RMSE (m/s)	Bais (m/s)	RMSE (m/s)	Bais (m/s)	RMSE (m/s)	Bais (m/s)	RMSE (m/s)	Bais (m/s)
MVE	1.803	1.695	-1.295	1.762	1.136	3.074	2.835	6.533	6.466	9.794	9.772
CyGNSSnet	1.405	0.917	-0.271	1.177	0.465	2.491	1.996	4.629	4.463	6.700	6.636
DDM-former	1.376	1.185	-0.796	1.070	-0.022	2.195	1.606	4.299	4.111	6.248	6.177
CyGNSSMsa	1.345	1.057	-0.431	1.139	0.104	2.158	1.561	4.055	3.873	6.208	6.133

As evidenced by the accuracy metrics presented in **Table 1**, the conventional MVE method exhibited the lowest overall accuracy due to the absence of distribution correction in its output predictions, particularly manifesting significantly higher RMSE ($\Delta > 1.904$ m/s) and bias ($\Delta > 2.003$ m/s) compared to deep learning approaches in wind speeds exceeding 12 m/s. Our proposed CyGNSSMsa achieved superior comprehensive performance with optimal global metrics, attaining an overall RMSE of 1.345 m/s. While CyGNSSMsa demonstrated marginally higher errors (RMSE: +0.069 m/s, Bias: +0.082 m/s) than DDM-former within the 4 - 8 m/s range. This performance enhancement stems from CyGNSSMsa’s global feature fusion mechanism, which synergistically integrates multi-scale spatial patterns and auxiliary constraints through attention-weighted feature recombination, thereby simultaneously improving both regional accuracy and systematic bias mitigation. The comparative error distributions across wind speed bins, as clearly illustrated in **Figure 4**, further substantiate these findings through quantitative visualization of error clustering characteristics.



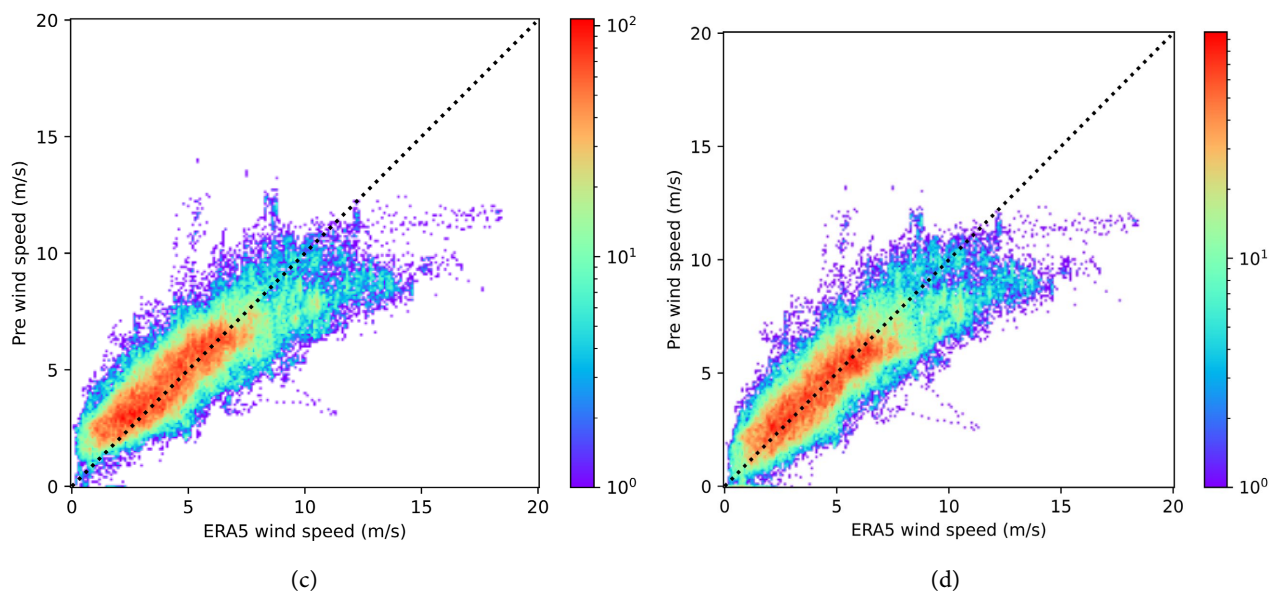


Figure 4. Density plots in log scale for four methods against ERA5 wind speeds. The colour bar measures samples per bin. Results of (a) MVE, (b) CyGNSSnet, (c) DDM-former, and (d) CyGNSSMsa. A 1:1 diagonal is shown as a black dotted line for reference

5. Conclusion

This study proposes CyGNSSMsa, an innovative wind speed retrieval model that synergistically integrates the dual-branch architecture of CyGNSSnet with multi-head self-attention (MSA) mechanisms. The proposed framework achieves state-of-the-art inversion accuracy, delivering an overall RMSE of 1.345 m/s. By deploying MSA layers to holistically interpret fused features from Delay-Doppler Maps (DDMs) and auxiliary parameters, CyGNSSMsa not only enhances precision but also reduces systematic bias across diverse wind regimes. The deepening convergence of deep learning and remote sensing technologies promises to address critical challenges in imbalanced wind speed distribution modeling through advanced data augmentation and physics-informed regularization.

Funding

This work was supported by the Key Program of Joint Fund of the National Natural Science Foundation of China and Shandong Province under Grant U22A20586, the Natural Science Foundation of Shandong Province under Grant ZR2022MD015, the Fundamental Research Funds for the Central Universities under Grant 24CX02030A, the National Natural Science Foundation of China under Grant 41701513, 61371189, and 41772350, and the Key Research and Development Program of Shandong Province under Grant 2019GGX101033.

Acknowledgements

We extend our sincere gratitude to NASA for the provision of CYGNSS data, as well as to the ECMWF for providing the ERA5 data.

Conflicts of Interest

The authors declare no conflicts of interest regarding the publication of this paper.

References

- [1] Clarizia, M.P., Ruf, C.S., Jales, P. and Gommenginger, C. (2014) Spaceborne GNSS-R Minimum Variance Wind Speed Estimator. *IEEE Transactions on Geoscience and Remote Sensing*, **52**, 6829-6843. <https://doi.org/10.1109/tgrs.2014.2303831>
- [2] Clarizia, M.P. and Ruf, C.S. (2016) Wind Speed Retrieval Algorithm for the Cyclone Global Navigation Satellite System (CYGNSS) Mission. *IEEE Transactions on Geoscience and Remote Sensing*, **54**, 4419-4432. <https://doi.org/10.1109/tgrs.2016.2541343>
- [3] Ruf, C.S. and Balasubramaniam, R. (2019) Development of the CYGNSS Geophysical Model Function for Wind Speed. *IEEE Journal of Selected Topics in Applied Earth Observations and Remote Sensing*, **12**, 66-77. <https://doi.org/10.1109/jstars.2018.2833075>
- [4] Reynolds, J., Clarizia, M.P. and Santi, E. (2020) Wind Speed Estimation from CYGNSS Using Artificial Neural Networks. *IEEE Journal of Selected Topics in Applied Earth Observations and Remote Sensing*, **13**, 708-716. <https://doi.org/10.1109/jstars.2020.2968156>
- [5] Liu, X., Bai, W., Xia, J., Huang, F., Yin, C., Sun, Y., *et al.* (2021) FA-RDN: A Hybrid Neural Network on GNSS-R Sea Surface Wind Speed Retrieval. *Remote Sensing*, **13**, Article No. 4820. <https://doi.org/10.3390/rs13234820>
- [6] Asgarimehr, M., Zhelavskaya, I., Foti, G., Reich, S. and Wickert, J. (2020) A GNSS-R Geophysical Model Function: Machine Learning for Wind Speed Retrievals. *IEEE Geoscience and Remote Sensing Letters*, **17**, 1333-1337. <https://doi.org/10.1109/lgrs.2019.2948566>
- [7] Liu, Y., Collett, I. and Morton, Y.J. (2019) Application of Neural Network to GNSS-R Wind Speed Retrieval. *IEEE Transactions on Geoscience and Remote Sensing*, **57**, 9756-9766. <https://doi.org/10.1109/tgrs.2019.2929002>
- [8] Asgarimehr, M., Arnold, C., Weigel, T., Ruf, C. and Wickert, J. (2022) GNSS Reflectometry Global Ocean Wind Speed Using Deep Learning: Development and Assessment of Cygnssnet. *Remote Sensing of Environment*, **269**, Article ID: 112801. <https://doi.org/10.1016/j.rse.2021.112801>
- [9] Guo, W., Du, H., Guo, C., Southwell, B.J., Cheong, J.W. and Dempster, A.G. (2022) Information Fusion for GNSS-R Wind Speed Retrieval Using Statistically Modified Convolutional Neural Network. *Remote Sensing of Environment*, **272**, Article ID: 112934. <https://doi.org/10.1016/j.rse.2022.112934>
- [10] Zhao, D., Heidler, K., Asgarimehr, M., Arnold, C., Xiao, T., Wickert, J., *et al.* (2023) Ddm-former: Transformer Networks for GNSS Reflectometry Global Ocean Wind Speed Estimation. *Remote Sensing of Environment*, **294**, Article ID: 113629. <https://doi.org/10.1016/j.rse.2023.113629>